RJC

RASĀYAN *J. Chem.*
Vol. 16 | No. 2 |905-920| April - June | 2023
ISSN: 0974-1496 | e-ISSN: 0976-0083 | CODEN: RJCABP
http://www.rasayanjournal.com
http://www.rasayanjournal.co.in

MOLECULAR STRUCTURE, EXPERIMENTAL AND THEORETICAL (HF, DFT) SPECTRAL ANALYSIS OF 3,4,5-TRIMETHOXYANILINE

Bandana Sharma[1,✉], Munish Kumar Yadav[2] and Shweta Prakash[3]
[1]Department of Applied Sciences & Humanities, Ajay Kumar Garg Engineering College, Ghaziabad-201009, Uttar Pradesh, India
[2]Department of Physics, Deva Nagri College, Meerut-250002-Uttar Pradesh, India
[3]Department of Applied Sciences & Humanities, Ajay Kumar Garg Engineering College, Ghaziabad-201009, Uttar Pradesh, India
✉Corresponding author: sharmabandana@akgec.ac.in

ABSTRACT
Experimental infrared and laser Raman spectra of 3,4,5-trimethoxyaniline were recorded in the first part of our investigation. Theoretically, using Hartree-Fock and density functional theory, structural properties and vibrational frequencies were estimated. The Hartree-Fock level spectral analysis was conducted using the HF/6-31+G(d,p) and HF/6-311++G(d,p) approaches. The B3LYP/6-31+G(d, p) technique was implemented to accomplish the DFT analysis. Comprehensive details of infrared, Raman intensity, scaled frequencies, reduced masses, and force constants are also presented in this paper. The vibrational experimental and theoretical findings are compared in the final section of our investigation using the 3D Gauss view visualization program. This paper also creates and provides Raman and IR spectra of 3,4,5-trimethoxy aniline using HF and DFT methodology.
Keywords: 3,4,5-trimethoxyaniline, FT-IR, Laser Raman Spectra, HF, and DFT Calculations.
RASĀYAN *J. Chem.*, Vol. 16, No.2, 2023

INTRODUCTION

Aniline and its by-products are the staple components in the production of various medicines like paracetamol, Tylenol, and acetaminophen. In the agricultural industry, they are used as pesticides and fungicides. A lot of materials made of anilines are used as antioxidants, activators, accelerators, and other chemicals for the rubber industry.[1-6] According to a report published by Global Information, Inc. (January 2022), the aniline market at the global level is expected to register a growth of approximately 5%.[7] Considering the tremendous applications of substituted anilines in different fields, their structural parameters and vibrational frequencies are of utmost importance. When quantum chemical calculations are used in synergy with spectral analysis, then exceptionally vital details about the identity and molecular structure of organic compounds can be established.[8-10] According to the information that we have gathered from the survey of the literature, it is clear that no computational analysis of 3,4,5-trimethoxy aniline has been reported so far.[1-10, 27-30] In order to get all the charismatic information about the molecule, knowledge of vibrational modes is of foremost importance. In the last two decades, after the recognition of theoretical methods as an effective tool for spectral analysis, many investigators have done a lot of research work on aromatic compounds with prominent industrial applications.[1-10,16-26] Sunderganeshan and his coworkers reported the experimental and quantum chemical calculations of 3,4-dimethoxy aniline.[1] Vibrational analysis of 4-chloro-N-methyl aniline, 2,6-dibromo-4-nitro aniline, 2-chloro-4-methyl aniline, and 2-chloro-6-methyl aniline is also reported in the literature.[2-4] Mehmat and his team published the experimental and theoretical study of 2-chloro-5-methyl aniline.[5] In addition, quantum chemical calculations of 2,6-dibromo-3-chloro-4-flouro aniline are also reported in the literature.[6] Recently, vibrational and electronic spectral analysis of xylene using DFT was reported by Emmanuel and his coworkers.[19] With each passing day, density functional theory is proving its worth in electronic, vibrational, and NMR analysis.[20–25, 28-30] Considering the importance of the mentioned compound, this investigation is actually an attempt to present the molecular structure, vibrational analysis, and other properties of 3,4,5-trimethoxy aniline. This is done

http://doi.org/10.31788/RJC.2023.1628371

with the assistance of computational analysis using HF and density functional theory along with experimental results. The present study on 3,4,5-trimethoxy aniline is divided into three parts:
(a) FT-IR and laser Raman spectral data recording and interpretation.
(b) Computation of structural parameters and vibrational frequencies using HF and DFT.
(c) A comparison of experimental and theoretical findings.

EXPERIMENTAL

Experimental Detail

With a stated purity of more than 99%, 3,4,5-tri methoxy aniline in the solid form was procured from Sigma Aldrich Chemical Pvt. Ltd., Germany, and was used in the same form. Figure-1 depicts the molecular composition and atom enumeration of 345TMA. The FT-IR spectra of the specified compound have been reported in the stated region of 4000-400 cm^{-1}. A Laser Raman spectrum has been documented from 2000 to 50 cm^{-1}. At USIC Delhi, an RXI-FT-IR Perkin-Elmer spectrometer was used to record the FT-IR spectra. The Renishaw inVia reflex micro-Raman spectrometer was adapted to record laser Raman spectra. Raman spectrum was recorded using an Argon ion laser with a 514 nm wavelength. FT-IR and laser Raman spectra of 3,4,5-TMA are exhibited in Figs.-2 and 3 respectively.

Computational Detail

The structural parameters of the 345TMA were optimized at Hartree-Fock and B3LYP levels using the Gaussian 03W program. Geometry optimization and vibrational frequency calculations at the HF level were performed at 6-31+G (d, p) and 6-311++G (d, p). DFT computations were performed at the B3LYP level using 6-31+G (d, p). Vibrational frequencies in conjunction with Raman and infrared intensities are obtained using these computational methods. Information on reduced masses, force constants, and depolarization ratios are also gathered and presented in tabular form in Tables 3, 4, and 5. The analysis of the theoretical data was done employing the 3D GAUSSVIEW visualization program. For the purpose of this paper's discussion, 6-31+G (d, p) is designated as level 1, while 6-311++G (d,p) is designated as level 2.

RESULTS AND DISCUSSION

Experimental Spectral Analysis

For the titled compound ($C_9H_{13}O_3N$), there are 26 atoms, which leads to 72 vibrational modes. These key vibrational frequencies are indeed active in IR and Raman.[11] Peaks corresponding to different vibrations in the infrared and Raman spectra generally complement each other. Vibrational spectra usually consist of a number of modes of discrete intensity at definite wave numbers. The observed FT-IR and Raman spectra are interpreted using the vibrational bands of molecules with similar structural properties. The fundamental criteria for vibrational assignments in our study are peak positions, shapes, and relative intensities.

NH_2 Group Vibrations

In principal aromatic amines, asymmetric and symmetric stretching modes show absorptions between 3300 and 3500 cm^{-1}.[12-15] Asymmetric stretching vibrations are substantially perceived at a lower wavelength than symmetric stretching. An infrared absorption peak at 3422 cm^{-1} is identified as asymmetric NH_2 stretching. Symmetric stretching of the NH_2 group is actually a pinnacle at 3320 cm^{-1} in vibrational IR spectra. According to Bellamy, the scissor vibrations of the amino group are between 1600 and 1700 cm^{-1}.[11] A peak at 1610 cm^{-1} in the vibrational infrared spectrum is designated as the NH_2 scissoring mode. Similarly, in the Raman spectrum, 1600 cm^{-1} is designated as the NH_2 scissoring vibrational mode.[1-6] According to a review of literature, NH_2 twisting vibration is typically found between 1060 and 1170 cm^{-1}.[1-3, 22-25] In the amino group, twisting frequency mode is found at 1136 cm^{-1} in the infrared range, whereas in the Raman Spectrum, it is identified at 1150 cm^{-1}. A strong peak at 625 cm^{-1} in the IR range and a Raman band at 606 cm^{-1} are associated with NH_2 wagging mode. Evans assigned the bands observed in the range of 420-460 cm^{-1} as the first overtone of the NH_2 torsional mode.[27] In laser Raman spectra, 126 cm^{-1} is identified as the NH_2 torsional mode. Previous investigators identified carbon-amino groups stretching from 1250 to 1340 cm^{-1}.[1-10] Peaks at 1236 and 1260 cm^{-1} in the infrared range are credited to carbon-amino group stretching vibration. The out-of-plane bending vibration of the carbon-amino group is connected with a strong peak in the laser

Raman range at 368 cm^{-1}, while the in-plane bending vibration is ascribed to a peak at 415 cm^{-1}. These vibrational assignments are in concurrence with earlier evidence.[1-15, 22-27]

Methoxy Group Vibrations

In the present investigation, three methoxy groups are present at the 3rd, 4th, and 5th positions. For the mentioned compound, 2790, 2795, 2800, 2820, 2835, and 2890 cm^{-1} of the IR spectrum are identified as methyl symmetric stretching vibrations. 2930, 3000, 3050, 3080, 3100, 3140, 3160, and 3180 cm^{-1} in the FT-IR spectrum of the aforementioned molecule are attributed to methyl asymmetric stretching vibrations. The strength of methoxy group bending vibrational modes is generally low to average in these regions. Peaks at 1363, 1370, 1380, and 1405 cm^{-1} in the Raman spectra are proposed as locations for the symmetric bending of the methoxy group. Similarly, 1380 cm^{-1} is allocated to symmetric bending. The Methoxy group is found to bend asymmetrically at 1440, 1450, 1460, and 1490 cm^{-1}. An infrared peak at 1459 cm^{-1} is earmarked for asymmetric bending of the methoxy group. Methyl rocking vibrations are identified at 1110, 1170, 1190, 1205, and 1220 cm^{-1} in the laser Raman spectrum. A band of weaker intensity in the IR spectrum at 1200 cm^{-1} is also assigned for methyl rocking vibration. The C-O stretching of the methoxy group in combination with methyl rocking vibrations appears to have low to powerful strength. This vibrational mode is often labeled "symmetric COC stretching. The interpretation of the entire IR and Raman spectra is done, and all the vibrational assignments are displayed in Table-1.

Table-1: Experimental FT-IR, laser-Raman frequencies, and vibrational assignments of 345TMA

IR (cm^{-1})	Raman (cm^{-1})	Assignments	IR (cm^{-1})	Raman (cm^{-1})	Assignments
	126	$\tau(NH_2)$	1136	1150	tNH_2 , α(C-H)
	180	$\tau(CH_3)$		1170	$\rho(CH_3)$, α(C-H)
	236	γ(C-NH_2), $\tau(CH_3)$		1190	$\rho(CH_3)$, α(C-H)
	290	$\tau(CH_3)$	1200	1205	$\rho(CH_3)$, α(C-H)
	320	γ(C-NH_2)		1220	$\rho(CH_3)$
	368	γ(C-NH_2)	1236	1260	ν(C-NH_2)
	405	γ(C-C-C)		1270	α (C-H)
	415	α(C-NH_2)		1290	α (C-H)
	460	γ(C-C-C)		1320	ν (C-O), α(C-H)
	470	γ(C-C-C)		1363	symmetric bending of OCH_3
	480	γ(C-C-C)	1380	1370	symmetric bending of OCH_3
526	527	γ(C-C-C)		1380	symmetric bending of OCH_3
	560	γ(C-C-C)		1405	symmetric bending of OCH_3
	595	δ(C-O)		1440	Asymmetric bending of OCH_3
625	606	ωNH_2		1450	Asymmetric bending of OCH_3
	640	δ(C-O)	1459	1460	ν(C-C), Asymmetric bending of OCH_3
	675	δ(C-O)		1490	Asymmetric bending of OCH_3
	685	δ(C-O)		1505	ν(C-C), Asymmetric bending of OCH_3
	710	γ(C-C-C)		1520	ν(C-C)
	730	γ(C-C-C)		1530	ν(C-C)
	738	γ(C-C-C)		1550	ν(C-C)
740	740	γ(C-C-C)		1575	ν(C-C)
	755	γ(C-H)		1585	ν(C-C)
	770	γ(C-H)	1610	1600	δ NH_2 ν(C-C)
780	777	α (C-C-C),γ(C-H)	2790		ν_s (CH_3)
805	810	α (C-C-C),γ(C-H)	2795		ν_s (CH_3)

	845	γ(C-H)	2800		ν_s (CH_3)
	870	α (C-C-C), γ (C-H)	2820		ν_s (CH_3)
	885	α (C-C-C),γ(C-H)	2835		ν_s (CH_3)
	890	α (C-C-C),γ(C-H)	2860		ν_s (CH_3)
	920	ν(C-O), ν (O-C)	2890		ν_s (CH_3)
	930	ν(C-O), ν (O-C)	2930		ν_{as} (CH_3)
940	940	ν(C-O), ν (O-C)	3000		ν_{as} (CH_3)
	960	ν(C-O), ν (O-C)	3050		ν_{as} (CH_3)
	980	ν(C-O), ν (O-C)	3080		ν_{as} (CH_3), ν(C-H)
	1005	ν(C-O), ν (O-C)	3100		ν_{as} (CH_3), ν(C-H)
995	1007	ring breathing	3140		ν_{as} (CH_3)
	1043	C-C-C trigonal bending, ν (O-C)	3160		ν_{as} (CH_3)
	1060	ν (C-O-C)	3180		ν_{as} (CH_3)
	1080	ν (C-O-C)	3211		ν_s (N-H)
	1095	ν (C-O-C)	3320		ν_s (N-H)
	1110	ρ(CH_3)	3422		ν_{as} (N-H)

Where ν–stretching, ν_s-symmetric stretching, ν_{as} -asymmetric stretching, α-in-plane bending, γ -out of plane bending, τ–torsion, ω-wagging, t-twisting, ρ-rocking, and δ-scissoring

C-C Vibrations

In benzene, aromatic carbon-carbon stretching is generally noticed from 1625 cm^{-1} to 1430 cm^{-1}. According to previous researchers, five bands of different intensities are observed in this range.[1-15] In the Raman laser spectrum of 345TMA, 1460, 1505, 1550, and 1600 cm^{-1} are allocated to aromatic carbon-carbon atom stretching. Similarly, 1459 and 1610 cm^{-1} are identified as carbon-carbon stretching vibrations in the IR spectrum. According to a literature survey, carbon trigonal bending, and ring breathing modes are perceived at 1010 and 992 cm^{-1}, respectively.[11-15] These vibrations interact significantly, and as a result of this interaction, energy will change. The current experiment detects ring breathing mode at 995 cm^{-1} in the IR band. In the laser Raman spectrum, a peak at 1043 cm^{-1} is picked as trigonal bending vibration.

C-H Vibrations

As it is evident from the molecular structure presented in Fig. 1, hydrogen atoms are present at the 2nd and 6th carbon atoms of the benzene ring. The presence of these hydrogen atoms leads to carbon-hydrogen in-plane as well as out-of-plane bending vibrations. These hydrogen atoms also lead the way for carbon-hydrogen stretching in 345TMA. As reported by earlier investigators, the characteristic region for carbon-hydrogen stretching of arenes is from 3100–3000 cm^{-1}.[1-20] So, IR peaks corresponding to 3080 and 3100 cm^{-1} are identified due to stretching of the carbon-hydrogen bond. By and large, in aromatic hydrocarbons, carbon-hydrogen out-of-plane bending is observed from 1000 cm^{-1} to 750 cm^{-1}. Earlier investigators found that carbon-hydrogen in-plane bending vibration mostly emerges from 1300 to 1000 cm^{-1}.[11-15] In infrared spectra, 1136, and 1200 cm^{-1} are finalized as carbon-hydrogen in-plane bending. Raman peaks at 1150, 1170, 1190, and 1205 cm^{-1} are also associated with the same mode. In the Raman spectrum of the present investigation, 405, 460, 470, 480, 527, and 560 cm^{-1} are designated as C-C-C out-of-plane bending vibrations. These are observed as weak bands in the Raman spectrum of the mentioned compound. A strong peak at 526 cm^{-1} in the infrared spectra of the mentioned compound is also labeled C-C-C, out of plane bending vibration. 595, 810, 870, 885, and 890 cm^{-1} are chosen for C-C-C in-plane bending in laser Raman spectra. 780 and 805 cm^{-1} are also put forth for this bending vibration in the infrared spectrum. Details of all the vibrational assignments which are related to 345TMA are presented in Table-1.

Computational Spectral Analysis

In order to support the experimental results, computational analysis was also done using HF theory at two different basis sets. The performance of the density functional theory for spectral analysis was also evaluated. The results of the experimental and theoretical investigation are compared and presented in tabular form in Table-7.

Structural Framework

Optimized structural parameters of 3,4,5-trimethoxy aniline were calculated and are recorded in Table 2. These parameters are in congruence with the atomic numbering system specified in Fig.-1. In a benzene ring, all the carbon atoms are sp^2 hybridized. Ideally, in the benzene ring, the bond lengths of all carbon-carbon bonds are the same because of the resonance. When hydrogen in the benzene ring is replaced with another substituent, then there is a change in various physical and chemical properties.[11-15] As it is clear from Table-2, there are structural changes in the benzene ring geometry because of the presence of methoxy and amino groups. These changes actually suggest an interaction between the benzene ring and the substituent. Bond lengths and bond angles in 345TMA have shown significant variations. But it is also evident here that bond length variations are very small as compared to angular changes. Aromatic C-C bond lengths range from 1.384 to 1.399 at the HF/level1, from 1.382 to 1.398 at the HF/level2, and from 1.398 to 1.411 Å at the DFT/level1. These bond length values are largely consistent with those of past studies.[1-15] The bond length for N9-H10 and N9-H11 bonds is the same (0.996 Å) at both levels of HF theory. Even in the DFT calculation, these two bonds are found to have the same bond length (1.011Å). There are three O-C bonds at the 3rd, 4th, and 5th positions for the titled compound. It is clear from Table-2 that at all levels, the O12-C23 bond length is the longest and the O14-C15 bond length is the smallest. All the other bond lengths are mentioned and presented in Table-2. The type of substituent and their position are also responsible for the trends of C-C-C bond angles. C-C-C bond angles range from 118.6 to 121.4 degrees at HF/levels 1 and 2, and from 118.5 to 121.4 degrees at the DFT level. The C-C-O bond angles at various positions range from 115.6 to 123.8° at HF/level 1 and HF/level 2. According to DFT calculations, this bond angle ranges from 115.4–124°. This structural data reflects the well-known trends reported earlier.[1-5]

Table-2: Structural Parameters (Bond Lengths, Bond Angles) of 345TMA at HF and DFT Levels

	Bond Length (Å)			Bond Angles (°)			
Bond	HF/ level1	HF/ level2	B3LYP/ level1	Bond angles	HF/ level1	HF/ level2	B3LYP/ level1
C2-C1	1.385	1.395	1.399	C6-C1-C2	119.6	119.6	119.5
C6-C1	1.397	1.383	1.407	C2-C1-N9	120.7	120.6	120.6
N9-C1	1.395	1.396	1.402	C3-C2-C1	119.8	120.1	120.1
C2-C3	1.390	1.385	1.398	C1-C2-H7	121.5	119.1	121.4
C2-H7	1.075	1.073	1.085	C6-C1-N9	119.7	119.8	119.9
C4-C3	1.384	1.398	1.401	C1-C6-C5	120.1	119.8	120.1
C3-O12	1.356	1.342	1.376	C1-C6-H8	119.1	121.4	119.2
C4-C5	1.399	1.382	1.411	C1-N9-10	114.7	113.4	115.1
C4-O13	1.360	1.359	1.378	C1-N9-H11	115	115.9	115.4
C5-C6	1.387	1.389	1.398	C3-C2-H7	118.8	120.7	118.5
C5-O14	1.344	1.355	1.367	C2-C3-C4	121.4	120.5	121.1
C6-H8	1.073	1.075	1.084	C2-C3-O12	118.4	123.8	117.8
N9-H10	0.996	0.996	1.011	C4-C3-O12	120.2	115.6	121
N9-H11	0.996	0.996	1.011	C5-C4-C3	118.6	118.6	118.5
O12-C23	1.413	1.411	1.435	C3-C4-O13	120.6	120.8	120.5
O13-C19	1.409	1.407	1.433	C3-O12-C23	116.2	120.3	115.8
O14-C15	1.401	1.399	1.421	C5-C4-O13	120.8	120.6	121
C15-H16	1.086	1.080	1.098	C4-C5-C6	120.5	121.4	120.7
C15-H17	1.080	1.086	1.091	C4-C5-O14	115.6	120.1	115.4
C15-H18	1.085	1.086	1.097	C4-O13-C19	115.6	115.6	114.7
C19-H20	1.084	1.086	1.095	C6-C5-O14	123.8	118.5	124
C19-H21	1.085	1.085	1.097	C5-C6-H8	120.8	118.8	120.7
C19-H22	1.082	1.082	1.092	C5-O14-C15	120.3	116	118.6
C23-H24	1.082	1.081	1.093	H10-N9-H11	111.5	111.1	111.7
C23-H25	1.081	1.082	1.092	O12-C23-H24	110.9	111	111.2
C23-H26	1.086	1.086	1.098	O12-C23-H25	106.3	106.5	105.9
Bond Angles (°)				O12-C23-H26	110.3	110.4	110.3

Bond angles	HF/ level1	HF/ level2	B3LYP/ level1	O13-C19-H20	110.8	110.7	110.9
H18-C15-H17	109.3	109.5	109.3	O13-C19-H21	110.7	110.9	110.7
H20-C19-H21	109.8	109.7	110	O13-C19-H22	106.7	106.8	106.2
H22-C19-H20	109.4	109.4	109.5	O14-C15-H16	111.4	111.5	111.5
H22-C19-H21	109.5	109.3	109.6	O14-C15-H17	106	106.1	105.7
H25-C23-H24	109.9	109.8	110	O14-C15-H18	111.3	111.3	111.4
H26-C23-H24	109.9	109.3	110	H17-C15-H16	109.2	109.1	109.4
H25-C23-H26	109.4	109.8	109.4	H18-C15-H16	109.6	109.2	109.5

Where level 1 is 6-31+G(d, p), and level 2 is 6-311++G(d, p).

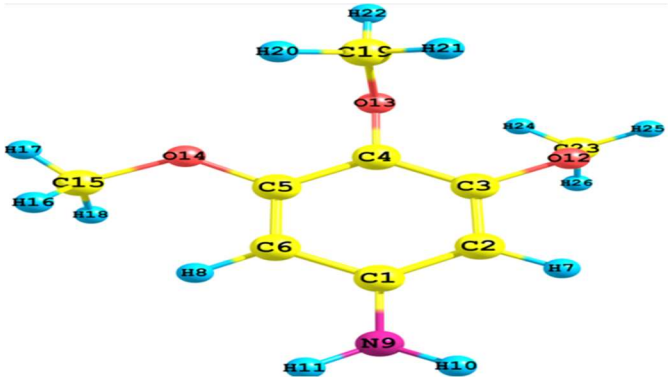

Fig.-1: Molecular Composition and Atomic Marking of 345TMA

Vibrational Analysis

The vibrationally moderated settings of 345 TMA were used for harmonic vibrational frequency computation. Assignments of vibrations can be achieved with a greater level of certainty using GaussView. The computed values have been utilized to stimulate infrared and Raman spectra. A comparison of experimental spectra and spectra based on the computational data reveals that the results are in close agreement with each other. However, the assignments of some of the peaks are in disagreement with the computed data. A few prominent computed vibrational frequencies and the discrepancies observed between experimental and computational data are discussed here. According to the vibrational analysis of 345TMA using HF and DFT methods, different thermodynamic functions are computed and presented in Table-6. This thermodynamical data provides the supporting information for future investigation.

A comparison between experimental and computational spectral analysis

Experimental and theoretical frequencies are compared and encapsulated in Table-7. A comprehensive discussion of some of the major observations is presented in this section. Asymmetric N-H stretching vibrations are visualized at scaled frequencies of 3482 and 3458 cm^{-1} at the HF level using HF/level1 and HF/level2, respectively. On a similar line, 3387 and 3372 cm^{-1} were picked as symmetric N-H stretching vibrations. According to DFT calculations, the asymmetric stretching of the nitrogen-hydrogen bond is spotted at 3530 cm^{-1} and symmetric stretching at 3429 cm^{-1}. It means, as far as N-H stretching is concerned, computational and experimental outcomes are in close concurrence with each other. At the experimental level, NH_2 wagging mode is identified at 625 and 606 cm^{-1}. Through the Gauss view visualization program, the same mode is spotted at 585, 593, and 565 cm^{-1} at HF/level1, HF/level 2, and B3LYP/level1 respectively. For the 345TMA, there are two hydrogen atoms present at the 2^{nd} and 6^{th} positions. At the theoretical level, with three different methods, scaled frequencies of 3010, 2991, and 3083 cm^{-1} are observed as C6-H8 stretching vibrations, whereas 2993, 2973, and 3071 cm^{-1} are identified as C2-H7 stretching vibrations. These theoretical results fit the experimental findings very well. At HF/level1, six scaled frequencies, 2943, 2942, 2927, 2913, 2899, and 2892 cm^{-1}, are assigned to asymmetric methyl group stretching with respect to three methyl groups, according to the Gauss view visualization program. At HF/level2, asymmetric stretching of the methyl group is located at 2922, 2920, 2907, 2891, 2878, and 2872 cm^{-1}. According to the DFT calculation, scaled frequencies of 3023, 3021, 3011, 2984, 2972, and 2956 cm^{-1} are assigned to the same stretching vibration. It means the experimental and theoretical findings are in

reconciliation with each other. Three CH_3 symmetric stretching vibrations are observed at 2839, 2838, and 2834 cm^{-1} for HF/level1 due to three methyl groups. According to HF/level2 computations, 2822, 2820, and 2817 cm^{-1} are also allocated to CH_3 symmetric stretching vibrations. For calculations based on density functional theory, 2904, 2904, and 2895 cm^{-1} are also assigned as CH_3 symmetric stretching. At the experimental level, CH_3 symmetric vibrations are found at 2890, 2860, 2835, 2820, 2800, 2795, and 2790 cm^{-1}.

CONCLUSION

Fourier transforms infrared and laser Raman spectra of 3,4,5-trimethoxy aniline have been recorded [Fig.-2,3] and a comprehensive interpretation of vibrational assignments has been done for the first time [Table-1]. HF and DFT methods were used to determine and analyze geometry [Table-2] and vibrational frequencies [Table-3 to 5]. Harmonic vibrational frequencies, bond lengths, bond angles, IR values, and Raman behaviors are all presented for the first time in this paper. The Raman and IR spectra were plotted and investigated at HF as well as DFT level [Fig.-4 To 9]. An authentic interpretation of vibrational bands was executed at both levels of computational analysis. In this investigation, vibrational frequency analysis employing HF and DFT methods coincides decently with experimental results. Most of the fundamental modes, like N-H stretching, C-H stretching, and C-C stretching, are discovered to be within the anticipated range [Table-1]. Most of the experimental results are found in sync with theoretical results [Table-7]. Therefore, the results presented in this paper for 3,4,5-trimethoxy aniline indicate that HF and DFT are dependable methods for the prediction of geometry as well as IR and Raman spectra. This provided more evidence that HF and DFT simulations are effective methods for deciphering the structure and vibrational spectra of molecules.

Table-3: The Theoretical Vibrational Parameters of 345TMA Calculated at HF/Level 1.

Unscaled Wavenumber	Scaled Wavenumber	IR Intensity	Raman activity	Reduced mass	Force constant	Depolar (P)	Depolar (U)
65	58	3	0	2.9863	0.0075	0.7444	0.8535
83	74	7	0	2.7011	0.0109	0.6582	0.7939
87	78	6	1	2.8622	0.0128	0.7480	0.8559
111	99	3	1	3.6652	0.0266	0.5404	0.7016
156	139	2	1	1.8679	0.0267	0.7493	0.8567
165	147	1	0	1.2298	0.0198	0.7451	0.8540
172	153	3	0	1.3141	0.0228	0.7496	0.8569
216	192	0	1	2.5920	0.0713	0.7328	0.8458
229	204	2	1	1.9219	0.0596	0.7081	0.8291
257	229	20	1	1.6161	0.0629	0.4282	0.5997
262	233	13	1	1.6571	0.0671	0.3700	0.5401
297	265	0	1	1.8471	0.0961	0.0486	0.0927
322	287	3	1	4.1303	0.2528	0.0611	0.1152
345	307	3	0	4.5238	0.3164	0.5913	0.7432
367	327	3	3	4.9525	0.3930	0.1217	0.2171
430	382	5	1	4.1469	0.4512	0.4391	0.6103
456	406	1	4	6.1581	0.7538	0.3622	0.5318
560	499	12	2	5.4019	0.9988	0.4086	0.5802
565	503	5	3	5.3171	1.0017	0.4111	0.5827
611	544	19	9	5.4791	1.2060	0.0864	0.1591
657	585	268	8	1.5688	0.3995	0.2412	0.3886
710	632	6	1	4.1049	1.2197	0.7500	0.8571
728	648	53	4	2.4181	0.7555	0.3777	0.5483
732	652	16	2	3.0704	0.9704	0.6374	0.7786
824	733	7	7	4.2471	1.6989	0.0329	0.0637
868	772	9	7	4.7116	2.0913	0.0919	0.1684
918	817	50	0	1.7148	0.8517	0.7448	0.8537
941	838	44	1	1.8240	0.9520	0.7493	0.8567

1037	923	19	3	5.4725	3.4695	0.7479	0.8558
1079	960	17	4	4.5215	3.1000	0.1263	0.2242
1146	1020	90	13	6.6792	5.1727	0.7263	0.8415
1171	1042	47	15	4.0064	3.2357	0.1200	0.2142
1176	1047	9	8	1.9707	1.6054	0.3239	0.4893
1251	1113	309	3	4.3655	4.0257	0.7444	0.8535
1278	1138	4	3	1.2621	1.2150	0.7482	0.8560
1280	1139	3	2	1.2610	1.2165	0.6482	0.7866
1281	1140	3	2	1.2700	1.2283	0.7458	0.8544
1289	1147	29	1	2.0098	1.9665	0.6368	0.7781
1295	1152	83	2	2.3244	2.2952	0.2185	0.3586
1316	1171	40	5	1.4540	1.4830	0.0714	0.1334
1334	1187	7	3	1.5712	1.6464	0.3077	0.4706
1337	1190	45	1	1.6422	1.7293	0.3085	0.4716
1381	1229	200	3	2.2298	2.5062	0.1303	0.2305
1392	1239	174	3	2.6155	2.9874	0.0909	0.1666
1507	1341	31	28	5.0920	6.8109	0.0243	0.0474
1591	1416	85	4	1.4430	2.1510	0.7339	0.8465
1602	1426	30	2	1.2294	1.8589	0.7299	0.8439
1619	1441	6	4	1.2321	1.9023	0.2587	0.4110
1620	1442	12	9	1.0512	1.6269	0.7177	0.8357
1622	1444	7	15	1.0703	1.6592	0.7384	0.8495
1628	1449	7	13	1.0473	1.6363	0.7487	0.8563
1632	1452	1	9	1.0572	1.6588	0.6681	0.8010
1637	1457	12	10	1.1157	1.7609	0.5800	0.7342
1638	1458	50	2	1.6919	2.6744	0.4787	0.6474
1639	1459	20	7	1.1390	1.8028	0.7006	0.8239
1685	1499	240	8	3.7945	6.3451	0.1326	0.2342
1781	1585	232	9	7.1211	13.3063	0.7376	0.8490
1798	1600	43	26	2.6262	5.0004	0.6987	0.8227
1817	1617	226	33	1.5621	3.0392	0.5501	0.7098
3184	2834	62	99	1.0343	6.1789	0.0196	0.0384
3188	2838	76	105	1.0315	6.1783	0.0086	0.0171
3190	2839	59	151	1.0374	6.2213	0.0240	0.0468
3250	2892	47	44	1.1068	6.8875	0.7362	0.8481
3258	2899	39	38	1.1063	6.9180	0.6929	0.8186
3273	2913	39	67	1.0972	6.9233	0.4364	0.6076
3289	2927	51	121	1.1046	7.0404	0.5258	0.6892
3306	2942	36	89	1.1076	7.1318	0.6430	0.7827
3306	2943	31	113	1.1019	7.0967	0.4456	0.6165
3363	2993	7	86	1.0928	7.2825	0.2894	0.4489
3382	3010	8	68	1.0910	7.3516	0.2703	0.4256
3806	3387	24	137	1.0492	8.9523	0.1248	0.2219
3912	3482	21	49	1.0990	9.9097	0.7500	0.8571

Where wavenumbers are in cm^{-1}, IR intensities in km mol^{-1}, Raman scattering activities in $Å^4amu^{-1}$, reduced masses in amu, and force constants are in m dyne$Å^{-1}$.

Table-4: The Theoretical Vibrational Parameters of 345TMA Calculated at HF/Level 2

Unscaled Wavenumber	Scaled Wavenumber	IR Intensity	Raman activity	Reduced mass	Force constant	Depolar (P)	Depolar (U)
65	58	3	0	3.0029	0.0076	0.7494	0.8568
84	75	8	0	2.6678	0.0111	0.6598	0.7950
88	79	5	1	2.9519	0.0136	0.7476	0.8555
112	99	3	1	3.6401	0.0267	0.5542	0.7132

157	139	3	1	2.1709	0.0314	0.7476	0.8556
166	148	1	0	1.1772	0.0192	0.7263	0.8414
173	154	2	0	1.2459	0.0219	0.7493	0.8567
215	192	0	1	2.4957	0.0682	0.7448	0.8538
229	204	2	1	1.9435	0.0600	0.7078	0.8289
255	227	24	0	1.1447	0.0437	0.5811	0.7350
261	232	8	1	2.8687	0.1153	0.3625	0.5321
297	264	0	0	1.8362	0.0954	0.0465	0.0889
323	287	2	1	4.2711	0.2625	0.0546	0.1035
343	305	2	0	4.4956	0.3119	0.5465	0.7068
367	326	3	3	5.0031	0.3961	0.1196	0.2136
428	381	4	1	4.1403	0.4479	0.3921	0.5633
456	406	1	4	6.2015	0.7599	0.3434	0.5112
561	499	10	3	5.6147	1.0412	0.3615	0.5310
566	504	6	2	5.1967	0.9822	0.4574	0.6277
611	544	10	10	5.908	1.3007	0.0811	0.1500
666	593	237	7	1.6392	0.4286	0.2483	0.3978
712	633	5	1	4.1714	1.2451	0.7317	0.8451
732	652	38	4	2.7804	0.8789	0.2595	0.4121
738	656	60	2	2.2579	0.7236	0.6441	0.7835
825	735	8	9	4.0641	1.6315	0.0345	0.0667
882	785	16	3	3.5822	1.6408	0.1371	0.2411
915	815	32	0	1.7724	0.8571	0.6284	0.7718
943	839	44	1	2.0904	1.0953	0.7376	0.8490
1035	921	19	2	5.3647	3.3853	0.7471	0.8552
1075	957	18	5	4.4643	3.0382	0.1134	0.2037
1144	1018	89	13	6.4627	4.9832	0.7305	0.8422
1167	1038	18	7	2.2237	1.7832	0.4217	0.5932
1168	1039	40	16	4.0529	3.2560	0.1233	0.2195
1245	1108	314	3	4.274	3.9011	0.7450	0.8539
1277	1136	3	2	1.2689	1.2184	0.7430	0.8525
1278	1137	3	3	1.2818	1.2334	0.5627	0.7202
1280	1139	2	2	1.2751	1.2302	0.7449	0.8538
1283	1142	40	1	1.9748	1.9147	0.6004	0.7503
1287	1146	85	2	2.2762	2.2220	0.2864	0.4453
1312	1168	50	5	1.4914	1.5128	0.0520	0.0989
1328	1182	1	2	1.5582	1.6193	0.4607	0.6308
1333	1186	44	2	1.5793	1.6532	0.1238	0.2203
1374	1223	194	3	2.1763	2.4201	0.1802	0.3054
1385	1233	167	3	2.5611	2.8958	0.1161	0.2080
1497	1332	31	28	5.1725	6.8299	0.0330	0.0639
1584	1410	88	3	1.4744	2.1790	0.7228	0.8391
1595	1420	29	1	1.2275	1.8406	0.7268	0.8418
1612	1435	9	4	1.2214	1.8701	0.1918	0.3219
1613	1436	12	6	1.0527	1.6144	0.7484	0.8561
1615	1438	7	12	1.0693	1.6436	0.7379	0.8492
1621	1443	8	11	1.0461	1.6199	0.7487	0.8563
1624	1446	1	7	1.0567	1.6428	0.6720	0.8038
1629	1450	9	8	1.1703	1.8307	0.5921	0.7438
1631	1451	46	2	1.4500	2.2718	0.3808	0.5516
1632	1452	29	5	1.1973	1.8778	0.7193	0.8367
1676	1492	242	8	3.7373	6.1873	0.1260	0.2238
1775	1580	226	9	7.1005	13.1793	0.7401	0.8507
1791	1594	48	27	2.7684	5.2314	0.7027	0.8254
1811	1612	209	34	1.5186	2.9388	0.5257	0.6892

3165	2817	60	104	1.0348	6.1086	0.0200	0.0392
3169	2820	74	107	1.0320	6.1058	0.0076	0.0151
3170	2822	53	167	1.0380	6.1469	0.0201	0.0395
3227	2872	46	42	1.1066	6.7883	0.7357	0.8477
3234	2878	39	36	1.1062	6.8161	0.6812	0.8104
3248	2891	37	62	1.0968	6.8169	0.4056	0.5771
3266	2907	51	118	1.1043	6.9387	0.5105	0.6759
3281	2920	35	86	1.1073	7.0219	0.5783	0.7328
3283	2922	36	111	1.1014	6.9924	0.4449	0.6158
3340	2973	7	83	1.0929	7.1854	0.2783	0.4354
3361	2991	8	65	1.0910	7.2593	0.2593	0.4119
3789	3372	23	143	1.0490	8.8722	0.1268	0.2251
3885	3458	19	48	1.0987	9.7718	0.7499	0.8571

Table-5: The Theoretical Vibrational Parameters of 345TMA Calculated at B3LYP/level 1

Unscaled Wavenumber	Scaled Wavenumber	IR Intensity	Raman activity	Reduced mass	Force constant	Depolar (P)	Depolar (U)
66	64	1	1	2.9009	0.0076	0.6729	0.8044
72	69	5	1	2.8119	0.0086	0.5829	0.7365
81	78	7	2	2.8704	0.0111	0.7315	0.8499
107	103	3	1	3.4561	0.0233	0.5135	0.6786
149	143	2	1	1.7832	0.0233	0.7492	0.8566
160	154	0	0	1.1214	0.0169	0.7450	0.8539
171	164	3	0	1.6278	0.0280	0.7191	0.8366
199	191	0	1	2.2613	0.0529	0.7114	0.8314
210	201	2	1	2.1302	0.0552	0.7367	0.8484
238	228	7	2	3.6184	0.1205	0.4328	0.6042
264	254	17	0	1.1539	0.0475	0.4730	0.6422
277	266	2	1	1.8304	0.0826	0.0672	0.1259
290	278	4	1	3.1716	0.1570	0.0977	0.1780
321	308	3	0	5.2190	0.3170	0.5286	0.6916
337	324	2	4	4.1440	0.2780	0.1297	0.2297
402	386	4	2	4.1914	0.3992	0.5460	0.7063
421	404	0	5	5.8958	0.6155	0.2560	0.4077
510	490	10	0	5.1014	0.7831	0.7192	0.8367
520	500	6	5	5.6056	0.8945	0.2669	0.4213
563	541	83	5	3.4319	0.6420	0.1602	0.2762
588	565	244	15	1.7068	0.3478	0.1920	0.3222
636	611	7	1	3.7623	0.8972	0.4880	0.6559
648	623	28	2	2.5003	0.6195	0.6695	0.8021
671	644	2	2	3.9553	1.0483	0.4027	0.5742
751	721	2	4	4.6787	1.5558	0.0277	0.0539
786	755	12	10	5.0725	1.8468	0.0735	0.1369
808	776	37	0	1.7103	0.6583	0.4151	0.5867
839	805	26	0	1.6755	0.6942	0.6833	0.8118
945	907	19	2	6.1339	3.2290	0.7489	0.8565
997	957	12	4	5.1675	3.0244	0.2341	0.3793
1033	992	77	15	8.2079	5.1621	0.7040	0.8263
1065	1023	38	22	3.7449	2.5033	0.0933	0.1707
1106	1062	59	1	1.5729	1.1345	0.6936	0.8191
1147	1101	239	3	3.0866	2.3928	0.5636	0.7209
1170	1123	2	2	1.2547	1.0120	0.7265	0.8416
1171	1124	1	2	1.2718	1.0280	0.7473	0.8554
1171	1125	3	3	1.2535	1.0136	0.5102	0.6756

1186	1139	27	3	2.1390	1.7734	0.2679	0.4226
1208	1160	16	3	1.3709	1.1785	0.1420	0.2487
1215	1166	48	2	1.5672	1.3628	0.5911	0.7430
1222	1173	50	3	1.5503	1.3644	0.7185	0.8362
1254	1204	128	11	2.5318	2.3450	0.1163	0.2084
1263	1213	143	4	1.9993	1.8804	0.2182	0.3582
1339	1285	16	1	7.2072	7.6133	0.7419	0.8518
1388	1333	12	41	5.0968	5.7873	0.0476	0.0908
1459	1401	47	4	1.3881	1.7409	0.7364	0.8482
1469	1410	22	3	1.2512	1.5914	0.6896	0.8163
1485	1426	1	7	1.2409	1.6122	0.2987	0.4600
1490	1430	13	10	1.0678	1.3968	0.7074	0.8286
1492	1432	10	14	1.0722	1.4057	0.7377	0.8491
1497	1437	8	13	1.0467	1.3824	0.7495	0.8568
1505	1445	50	2	2.1806	2.9090	0.7082	0.8292
1508	1447	3	8	1.0505	1.4070	0.6757	0.8064
1508	1448	47	8	1.0845	1.4530	0.5026	0.6690
1516	1455	3	7	1.0591	1.4338	0.7079	0.8290
1535	1473	161	11	3.3053	4.5862	0.2417	0.3893
1628	1563	151	8	7.3666	11.5049	0.7484	0.8561
1650	1584	66	36	2.9277	4.6989	0.7115	0.8314
1667	1601	194	35	1.4530	2.3798	0.5659	0.7227
3016	2895	65	136	1.0344	5.5420	0.0268	0.0523
3025	2904	109	34	1.0363	5.5857	0.2396	0.3866
3025	2904	36	259	1.0333	5.5725	0.0079	0.0157
3079	2956	39	60	1.1060	6.1772	0.7375	0.8489
3096	2972	29	45	1.1055	6.2442	0.6777	0.8079
3109	2984	30	67	1.0960	6.2406	0.4423	0.6133
3137	3011	32	138	1.1030	6.3941	0.5096	0.6752
3147	3021	20	103	1.1060	6.4531	0.5652	0.7222
3149	3023	21	121	1.0997	6.4257	0.4735	0.6427
3199	3071	7	98	1.0911	6.5805	0.2905	0.4502
3212	3083	8	77	1.0894	6.6207	0.2409	0.3883
3572	3429	16	213	1.0479	7.8766	0.1457	0.2544
3677	3530	15	60	1.0987	8.7532	0.7497	0.8570

Table-6: Theoretically Computed Parameters of 345TMA

Specification	HF		DFT
	HF/level1	HF/level2	B3LYP/level1
Total Energy(a.u.)	-627.4044075	-627.5318729	-631.202651
Zero-Point Energy (kcal/ mol)	143.95879	143.33576	134.12412
Rotational Constants (GHz)	0.89969	0.90067	0.88447
	0.77792	0.77939	0.76599
	0.45004	0.45107	0.44117
Dipole Moment (debyes)	2.6008	2.5727	2.7466
Entropy(cal/mol-Kelvin)			
Total	113.218	113.119	116.332
Trans.	41.521	41.521	41.521
Rot.	31.301	31.296	31.353
Vib.	40.396	40.302	43.458
Thermal energy (kcal/mol)			
Total	152.283	151.654	142.932
Trans.	0.889	0.889	0.889

Rot.	0.889	0.889	0.889
Vib.	150.505	149.876	141.154
Specific Heat(cal/mol-Kelvin)			
Total	47.903	47.906	51.222
Trans.	2.981	2.981	2.981
Rot.	2.981	2.981	2.981
Vib.	41.941	41.944	45.260

Where trans. denotes translation, rot. denotes rotation, and vib. denotes vibration.

Table-7: Analysis of the Vibrational Frequencies of 345TMA using Both Experimental and Computational Data

Experimental		Computational						Vibrational Assignment
		HF/level1		HF/level 2		B3LYP/level 1		
IR	Raman	Unscaled	Scaled	Unscaled	Scaled	Unscaled	Scaled	
		65	58	65	58	66	64	τ (CH_3)
		83	74	84	75	72	69	τ (CH_3)
		87	78	88	79	81	78	τ (CH_3)
		111	99	112	99	107	103	τ (CH_3)
		156	139	157	139	149	143	τ (CH_3)
		165	147	166	148	160	154	τ (CH_3)
	180	172	153	173	154	171	164	τ (CH_3)
		216	192	215	192	199	191	τ (NH_2)
	236	229	204	229	204	210	201	τ (CH_3)
	368	257	229	255	227	238	228	γ(C-NH_2)
		262	233	261	232	264	254	τ (NH_2)
		297	265	297	264	277	266	τ (CH_3)
		322	287	323	287	290	278	C-O-C bending
		345	307	343	305	321	308	C-O-C bending, α(C-NH_2)
		367	327	367	326	337	324	C-O-C bending
		430	382	428	381	402	386	C-O-C bending
		456	406	456	406	421	404	C-O-C bending
		560	499	561	499	510	490	C-O-C bending
		565	503	566	504	520	500	C-O-C bending
		611	544	611	544	563	541	C-O-C bending
625	606	657	585	666	593	588	565	ω(NH_2)
	640	710	632	712	633	636	611	γ(C-H), δ(C-O)
		728	648	732	652	648	623	γ(C-H), ω(NH_2)
		732	652	738	656	671	644	γ(C-H), δ(C-O)
		824	733	825	735	751	721	γ(C-H), α(C-C-C)
780	777	868	772	882	785	786	755	γ(C-H), γ(C-C-C)
805	810	918	817	915	815	808	776	γ(C-H)
	845	941	838	943	839	839	805	γ(C-H)
	920	1037	923	1035	921	945	907	ν(C-O-C)
	960	1079	960	1075	957	997	957	ν (C-O-C), α(C-H), ν (C-NH_2)
	1005	1146	1020	1144	1018	1033	992	ν(O-CH_3)
	1043	1171	1042	1167	1038	1065	1023	ν(O-CH_3), α(C-H)
		1176	1047	1168	1039	1106	1062	t(NH_2), α(C-H)
		1251	1113	1245	1108	1147	1101	ν(O-CH_3)
		1278	1138	1277	1136	1170	1123	ρCH_3
		1280	1139	1278	1137	1171	1124	ρCH_3
	1110	1281	1140	1280	1139	1171	1125	ρCH_3
1136		1289	1147	1283	1142	1186	1139	t(NH_2)
	1150	1295	1152	1287	1146	1208	1160	t(NH_2), α(C-H)
	1170	1316	1171	1312	1168	1215	1166	ρCH_3, α(C-H)

		1334	1187	1328	1182	1222	1173	ρCH_3, α(C-H)
	1190	1337	1190	1333	1186	1254	1204	ρCH_3, α(C-H)
		1381	1229	1374	1223	1263	1213	α (C-H)
		1392	1239	1385	1233	1339	1285	ν(C-O), α (C-H)
		1507	1341	1497	1332	1388	1333	ν(C-O), ν(C-NH_2)
1380	1370	1591	1416	1584	1410	1459	1401	symmetric bending of OCH_3, α (C-H)
	1380	1602	1426	1595	1420	1469	1410	symmetric bending of OCH_3
	1405	1619	1441	1612	1435	1485	1426	symmetric bending of OCH_3
	1440	1620	1442	1613	1436	1490	1430	asymmetric bending of OCH_3
		1622	1444	1615	1438	1492	1432	asymmetric bending of OCH_3
	1450	1628	1449	1621	1443	1497	1437	asymmetric bending of OCH_3
		1632	1452	1624	1446	1505	1445	asymmetric bending of OCH_3
		1637	1457	1629	1450	1508	1447	asymmetric bending of OCH_3
1459	1460	1638	1458	1631	1451	1508	1448	asymmetric bending of OCH_3, α (C-H)
		1639	1459	1632	1452	1516	1455	asymmetric bending of OCH_3
		1685	1499	1676	1492	1535	1473	ν(C-C), α(C-H)
	1575	1781	1585	1775	1580	1628	1563	ν(C-C), α(C-C-C)
	1585	1798	1600	1791	1594	1650	1584	δ(NH_2), α(C-H),ν(C-C)
1610	1600	1817	1617	1811	1612	1667	1601	δ(NH_2)
2800		3184	2834	3165	2817	3016	2895	ν_s(CH_3)
2820		3188	2838	3169	2820	3025	2904	ν_s(CH_3)
2835		3190	2839	3170	2822	3025	2904	ν_s(CH_3)
		3250	2892	3227	2872	3079	2956	ν_{as}(CH_3)
		3258	2899	3234	2878	3096	2972	ν_{as}(CH_3)
		3273	2913	3248	2891	3109	2984	ν_{as}(CH_3)
		3289	2927	3266	2907	3137	3011	ν_{as}(CH_3)
2930		3306	2942	3281	2920	3147	3021	ν_{as}(CH_3)
3000		3306	2943	3283	2922	3149	3023	ν_{as}(CH_3)
3080		3363	2993	3340	2973	3199	3071	ν(C-H), ν_{as} (CH_3)
3100		3382	3010	3361	2991	3212	3083	ν(C-H), ν_{as} (CH_3)
3320		3806	3387	3789	3372	3572	3429	ν_s(N-H)
3422		3912	3482	3885	3458	3677	3530	ν_{as}(N-H)

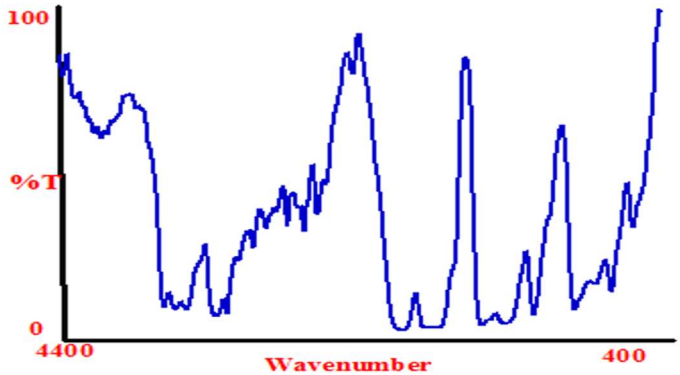

Fig.-2: Experimental FT-IR Spectrum of 345TMA in KBr Pallets

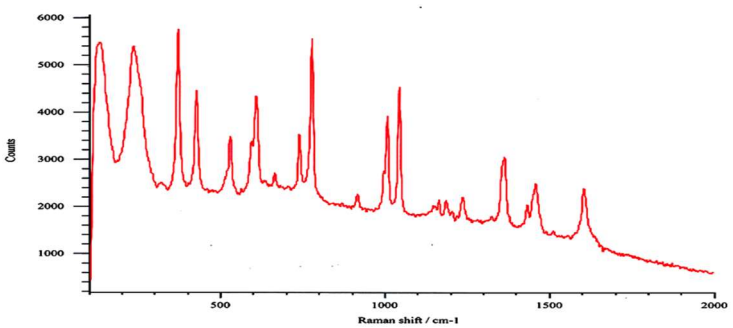

Fig.-3: Laser Raman Spectrum of 345TMA

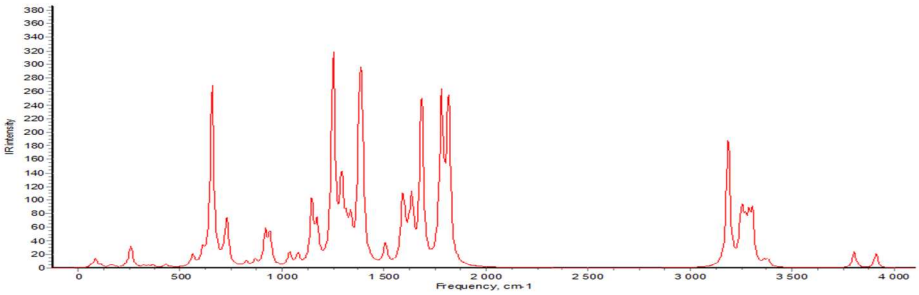

Fig.-4: Theoretical IR Spectrum of 345TMA: HF/6-31+G (d, p)

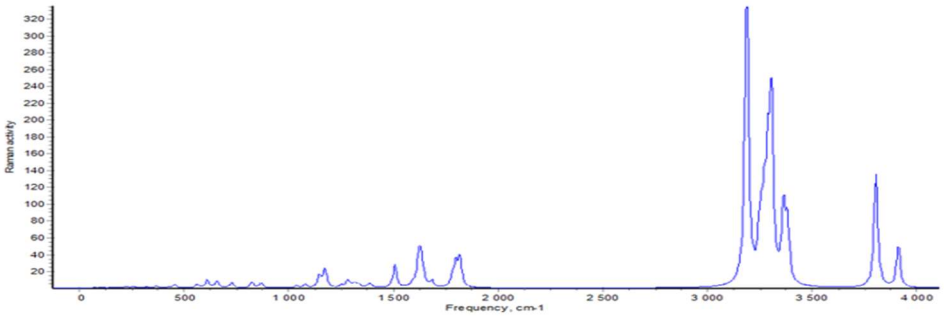

Fig.-5**:** Theoretical Raman spectrum of 345TMA: HF/6-31+G (d, p)

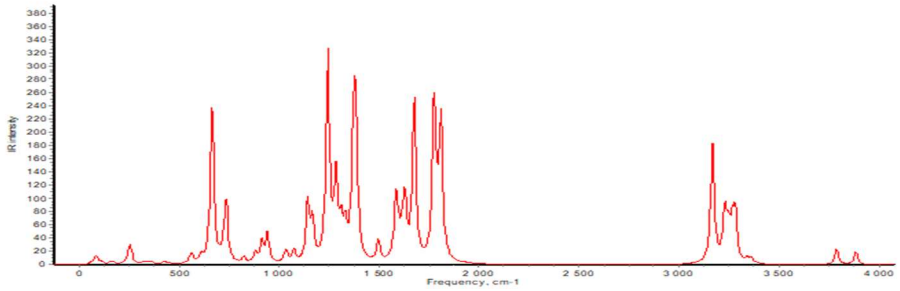

Fig.-6**:** Theoretical IR Spectrum of 345TMA: HF/6-311++G (d, p)

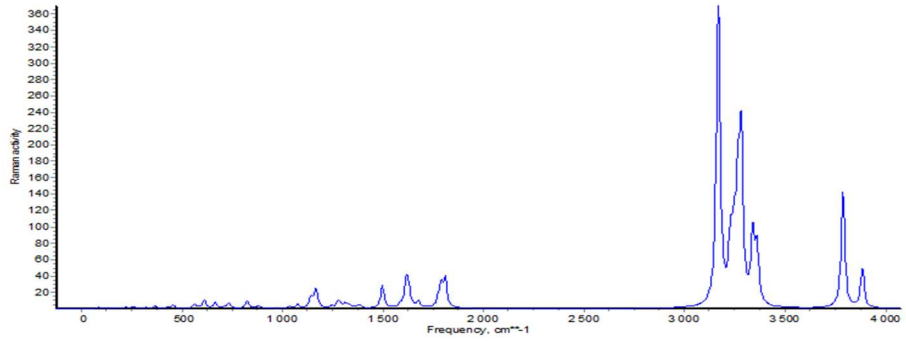

Fig.-7**:** Theoretical Raman Spectrum of 345TMA: HF/6-311++G (d, p)

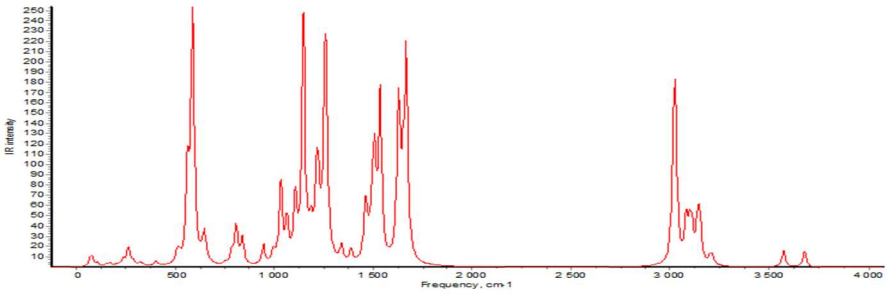

Fig.-8: Theoretical IR Spectrum of 345TMA: B3LYP/6-31+G (d, p)

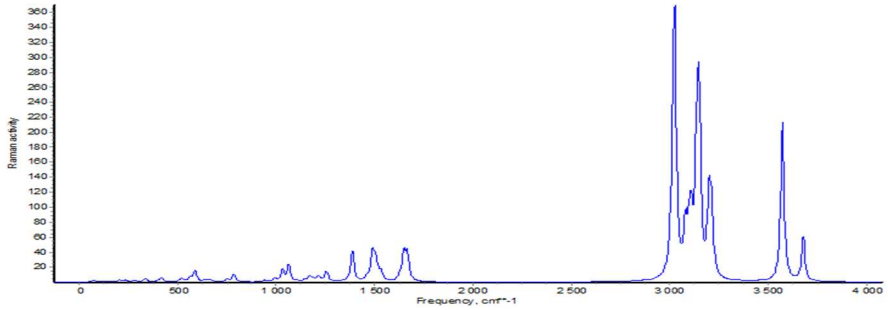

Fig.-9: Theoretical Raman Spectra of 345TMA: B3LYP/6-31+G (d, p)

CONFLICT OF INTERESTS

The authors declare that there is no conflict of interest.

AUTHOR CONTRIBUTIONS

All the authors contributed significantly to this manuscript, participated in reviewing/editing, and approved the final draft for publication. The research profile of the authors can be verified from their ORCID ids, given below:

Bandana Sharma https://orcid.org/0000-0002-8401-1254
Munish Kumar Yadav https://orcid.org/0000-0003-1540-9733
Shweta Prakash https://orcid.org/0009-0004-0615-2870

REFERENCES

1. N. Sundaraganesan, M. Priya, C. Meganathan, B. D. Joshua, and J. P. Cornard, *Spectrochimica Acta Part A: Molecular and Biomolecular Spectroscopy*, **70(1)**, 50(2008), https://doi.org/10.1016/j.saa.2007.07.026
2. A. Usha Rani, N. Sundaraganesan, M. Kurt, M. Cinar, M. Karabacak, *Spectrochimica Acta Part A: Molecular and Biomolecular Spectroscopy*, **75(5)**, 1523(2010), https://doi.org/10.1016/j.saa.2010.02.010
3. V. Krishnakumar, V. Balachandran, *Spectrochimica Acta Part A: Molecular and Biomolecular Spectroscopy*, **61(8)**, 1811(2005), https://doi.org/10.1016/j.saa.2004.07.012
4. V. Arjunan, S. Mohan, *Spectrochimica Acta Part A: Molecular and Biomolecular Spectroscopy*, **72(2)**, 436(2009), https://doi.org/10.1016/j.saa.2008.10.017
5. M. Karabacak, D. Karagöz, and M. Kurt, *Journal of Molecular Structure*, **892(1-3)**, 25(2008), https://doi.org/10.1016/j.molstruc.2008.04.054
6. A. Eşme and S. G. Sağdınç, *Journal of Applied Spectroscopy*, **84**, 1098(2018), https://doi.org/10.1007/s10812-018-0594-8

7. Global Information, Inc. (January 2022)
8. D. Mahadevan, S. Periandy, and S. Ramalingam, *Spectrochimica Acta Part A: Molecular and Biomolecular Spectroscopy*, **79(5)**, 962(2011), https://doi.org/10.1016/j.saa.2011.04.003
9. P. B. Nagabalasubramanian, S. Periandy, and S. Mohan, *Spectrochimica Acta Part A: Molecular and Biomolecular Spectroscopy*, **77(1)**, 150(2010), https://doi:10.1016/j.saa.2010.04.043
10. P. B. Nagabalasubramanian and S. Periandy, *Spectrochimica Acta Part A: Molecular and Biomolecular Spectroscopy*, **77(5)**, 1099(2010), https://doi:10.1016/j.saa.2010.09.002
11. L. J. Bellamy, The Infrared Spectra of the Complex Molecules, Wiley, New York, (1959)
12. C. N. Banwell and E. M. McCash, Fundamentals of Molecular Spectroscopy, 4th edition, Tata Mc Graw Hill Publishing Company Ltd., New Delhi, (1997)
13. N. P. G. Roeges, A Guide to the Complete Interpretation of Infrared Spectra of Organic Structures, Wiley, New York, (1994)
14. N. B. Colthup, Introduction to Infrared and Raman Spectroscopy, 2nd edition, Academic Press, New York, San Francisco, London, (1975)
15. G. Socrates, Infrared and Raman Characteristic Group Frequencies, 1st edition, John Wiley, New York, (1980)
16. E. Kavitha, N. Sundarganesan, S. Sebastian, *Indian Journal of Pure and Applied Physics*, **48**, 20(2010)
17. U. John and K. P. R. Nair, *Spectrochimica Acta Part A: Molecular and Biomolecular Spectroscopy*, **60(10)**, 2337(2004), https://doi.org/10.1016/j.saa.2003.12.007
18. J. R. Durig and F. F. D. Daeyaert, *Journal of Molecular Structure: THEOCHEM*, **261**, 133(1992), https://doi.org/10.1016/0166-1280(92)87072-8
19. E. A. Bisong, H. Louis, T. O. Unimuke, J. O. Odey, E. I. Ubana, M. M. Edim, F. T. Tizhe, J. A. Agwupuye, P. M. Utsu, *Heliyon,* **6(12)**, 2020, e05783, https://doi.org/10.1016/j.heliyon.2020.e05783
20. E. Yabalak, H. Dal, and H. Arslan, *Journal of Molecular Structure*, **1179**, 540(2019), https://doi.org/10.1016/j.molstruc.2018.10.079
21. A. Frisch, A. B. Nielson, and A. J. Holder, GaussView User Manual, Gaussian, Incorp, Pittsburgh, (2000)
22. A. K. Rai, S. Kumar, and A. Rai, *Vibrational Spectroscopy*, **42(2)**, 397(2006), https://doi.org/10.1016/j.vibspec.2006.05.033
23. M. Arivazhagan and D. Anitha Rexalin, *Spectrochimica Acta Part A: Molecular and Biomolecular Spectroscopy.* **96**, 668(2012), https://doi.org/10.1016/j.saa.2012.07.040
24. G. Shakila and H. Saleem, *IOSR Journal of Applied Physics*, **9(4)**, 42(2017), https://doi.org/10.9790/4861-0904024258
25. V. Kumar, Y. Panikar, M., A. Palafox, J. K. Vats, I. Kostova, K. Lang, V. K. Rastogi, *Indian Journal of Pure & Applied Phys*ics, **48**, 85(2010)
26. B. Revathia, V. Balachandrana, B. Rajab, and K. Anithac, *Indian Journal of Pure & Applied Phys*ics, **55**, 43(2017), https://doi.org/10.56042/ijpap.v55i01.13842
27. J. C. Evans, *Spectrochimica Acta*, **16(4)**, 428(1960), https://doi.org/10.1016/0371-1951(60)80037-9
28. S. Guidara, H. Feki, Y. Abid, *Spectrochimica Acta Part A: Molecular and Biomolecular Spectroscopy*, **133**, 856(2014), https://doi.org/10.1016/j.saa.2014.06.021
29. E. Yabalak, H. Dal, H. Arslan, *Journal of Molecular Structure*, **1179**, 540(2019), https://doi.org/10.1016/j.molstruc.2018.10.079
30. M. Rouhani, *Heliyon*, **5(10)**, 2019, e02518, https://doi.org/10.1016/j.heliyon.2019.e02518

[RJC-8371/2023]